

## Canonical correlation analysis based fault diagnosis method for structural monitoring sensor networks

Hai-Bin Huang<sup>1</sup>, Ting-Hua Yi<sup>\*1</sup> and Hong-Nan Li<sup>1,2</sup>

<sup>1</sup>School of Civil Engineering, Dalian University of Technology, Dalian 116023, China

<sup>2</sup>School of Civil Engineering, Shenyang Jianzhu University, Shenyang 110168, China

(Received November 30, 2015, Revised April 4, 2016, Accepted April 10, 2016)

**Abstract.** The health conditions of in-service civil infrastructures can be evaluated by employing structural health monitoring technology. A reliable health evaluation result depends heavily on the quality of the data collected from the structural monitoring sensor network. Hence, the problem of sensor fault diagnosis has gained considerable attention in recent years. In this paper, an innovative sensor fault diagnosis method that focuses on fault detection and isolation stages has been proposed. The dynamic or auto-regressive characteristic is firstly utilized to build a multivariable statistical model that measures the correlations of the currently collected structural responses and the future possible ones in combination with the canonical correlation analysis. Two different fault detection statistics are then defined based on the above multivariable statistical model for deciding whether a fault or failure occurred in the sensor network. After that, two corresponding fault isolation indices are deduced through the contribution analysis methodology to identify the faulty sensor. Case studies, using a benchmark structure developed for bridge health monitoring, are considered in the research and demonstrate the superiority of the new proposed sensor fault diagnosis method over the traditional principal component analysis-based and the dynamic principal component analysis-based methods.

**Keywords:** structural health monitoring; sensor fault diagnosis; canonical correlation analysis; dynamic or auto-regressive characteristic; contribution analysis

### 1. Introduction

Over the past two decades, advances in sensor technology and signal-processing techniques have witnessed the rapid development of structural health monitoring (SHM) methodology (Worden *et al.* 2008, Ni *et al.* 2010, Ni *et al.* 2012, Yi *et al.* 2013a, Li *et al.* 2014, Dessi and Camerlengo 2015). The health conditions of in-service civil infrastructures can be evaluated by employing the SHM system, after that some proper treating measures are implemented to ensure the safe and sustainable operation of the monitored infrastructure. Among various SHM technologies, the vibration based one has been most widely studied for estimating the structural damage information and modal parameters (Li and Law 2012, Yi *et al.* 2013b, Li *et al.* 2015, Rahbari *et al.* 2015, Yamaguchi *et al.* 2015). In principle, the performance of an SHM system

---

\*Corresponding author, Professor, E-mail: [yth@dlut.edu.cn](mailto:yth@dlut.edu.cn)

depends heavily on the quantity and quality of the health-monitoring data acquired from the sensor network. Hence, the problem of optimal sensor placement has gained considerable attention in recent years (Yi *et al.* 2011, Soman *et al.* 2014, Yi *et al.* 2015). Based on the optimal sensor placement technique, the sensor network can be properly installed to the civil infrastructure to guarantee the quantity of the health-monitoring data. Another technique which is called the sensor fault diagnosis method, however, also deserves significant attention along with the functional degradation and disabler of the sensors installed to the monitored structure. As an important practical aspect of SHM, sensor fault diagnosis method can be used for showing whether the quality of the health-monitoring data collected from the sensor network is eligible for the subsequent structural health evaluation procedure.

Unfortunately, limited attention has been paid to the sensor fault diagnosis technology, which is well studied in fault tolerant control area of smart civil structures (Wang and Song 2011, Huo *et al.* 2012, Pereira and Serpa 2015), by researchers in the SHM field. Generally, sensor fault diagnosis technique includes two major sub-procedures, namely the sensor fault detection sub-procedure used to decide whether a fault or failure occurred in the sensor network and the sensor fault isolation sub-procedure employed to identify the faulty sensor among the sensor network. Considering that errors introduced by sensor faults cause a loss of performance and erroneous conclusions, Abdelghani and Friswell (2004) proposed two residual generation schemes. These are the modal filtering technique and the parity space technique of monitoring the additive type of sensor faults. The efficacy of these two approaches was then demonstrated on a simulated cantilevered beam and also on an experimental sub-frame structure. Abdelghani and Friswell (2007) studied another type of sensor fault, namely multiplicative faults. In this research, a new residual generation and evaluation technique for sensor fault detection was proposed, and a correlation index was then established to isolate the faulty sensor. This approach had been experimentally validated on a sub-frame structure. Kerschen *et al.* (2005) presented a data-driven sensor validation approach for SHM systems by applying principal component analysis (PCA) to model the structural monitoring data. They used the angle between the principal subspaces as the feature for sensor fault detection. The isolation of the sensor fault was implemented by removing one sensor in turn, and the faulty sensor was the removed sensor in the case with the minimum angle. Sharifi *et al.* (2010) proposed a PCA-based sensor fault diagnosis method in the residual subspace rather than the principal subspace specifically for smart structures. They computed the fault probability of each sensor with a Bayesian probabilistic decision to analyze these residuals. As single or multiple sensors could be estimated from the remaining sensors with sufficient training data from the sensor network, Kullaa (2010) proposed a method for sensor validation, i.e., sensor fault detection, isolation and correction, using minimum mean square error estimation. The combination of the spatial and temporal correlations of the sensor output data improved the performance of this approach. Considering the shortcomings of using only one latent-variable-based monitoring method (primarily the PCA-based technique), Hernandez-Garcia and Masri (2014) applied three latent-variable-based statistical monitoring approaches (the PCA, the independent component analysis, and the modified independent component analysis-based approaches) to detect and isolate faulty sensors in the SHM system. Hotelling's  $T^2$  or  $I^2$  statistic and the squared prediction error (SPE) statistic were used for each of these three methods. They were evaluated and compared using case studies from an analytical truss model and a cable-supported bridge. Rather than using physical redundancy, Smarsly and Law (2014) presented an autonomous and fully decentralized approach toward sensor fault diagnosis in wireless SHM systems. They used analytical redundancy, which is the inherent information in the multivariate

redundant measurement system. Each sensor output in this method was predicted using the output of other sensors based on the back propagation neural network. This was embedded in each of the wireless sensor nodes installed on the monitored structure, and the residuals between the real and predicted sensor output values were used to autonomously detect and isolate the bias and drift sensor faults in real time. Huang *et al.* (2015) proposed a sensor fault diagnosis method based on statistical hypothesis test and the missing variable approach. In this research, the sensor fault detection process was first represented as a statistical hypothesis-testing problem, after which two fault detectors were deduced through the Bayesian linear model and the generalized likelihood ratio test method to examine whether a fault occurred in the sensor network. The missing variable approach was finally used to build a fault isolation index to identify the faulty sensor. Multivariate statistical process control-based fault diagnosis technology has been widely studied in many fields, such as chemical process monitoring (Yin *et al.* 2012, Lau *et al.* 2013). The multivariate statistical process control methodology has immense potential particularly in sensor fault diagnosis for SHM systems, due to that the structural response is monitored inherently as a multivariate measurement process by the professionally designed sensor network.

The PCA-based multivariate statistical process control is perhaps the most popular and broadly studied method for its theoretical simplicity and computational efficiency for model building. Nevertheless, the potential drawback of this method remains in two aspects: (1) it does not take the dynamic characteristic into account; (2) the two traditional fault detection statistics of it, i.e., the  $T^2$  statistic and the SPE statistic, are not sensitive to small or tiny faults. This paper presents a sensor fault diagnosis method, which takes the dynamic characteristic hidden in the health-monitoring data into account, based on the canonical correlation analysis (CCA) technique. To our best knowledge, this is the first application of CCA to harness the dynamic properties for developing sensor fault diagnosis method. The remainder of the paper is organized as follows. Section 2 briefly reviews the theoretical background of CCA. Section 3 first illustrates the dynamic characteristic of the structural accelerometer measurements through the auto-regressive model, and then employs the CCA technique for dynamic modeling of the health-monitoring data. Based on this, two statistics are built for sensor fault detection and two corresponding fault isolation indices are deduced to identify the faulty sensor. Section 4 elaborates the implementation process of the proposed sensor fault diagnosis method. Section 5 considers case studies using the benchmark structure developed for bridge health monitoring to validate the effectiveness and capability of the proposed sensor fault diagnosis methodology. Section 6 gives the summaries and conclusions in detail.

## 2. Brief review of canonical correlation analysis

CCA is a statistical technique to measure the underlying correlation between two sets of multidimensional variables. For the sake of completeness, a brief theoretical background of CCA is given in this section (Hardoon *et al.* 2004, Correa *et al.* 2010, Huang *et al.* 2010, Sweeney *et al.* 2013).

Considering two multidimensional datasets  $\mathbf{X}^a$  and  $\mathbf{X}^b$  with the same number of sampling points, CCA measures their linear relationships through their auto-covariance and cross-covariance matrices. In CCA, the dimensions  $m_a$  and  $m_b$  of the respective data vectors  $\mathbf{x}^a \in \mathbf{X}^a$  and  $\mathbf{x}^b \in \mathbf{X}^b$  can be different, but they are both assumed to be zero-mean processes. In case they are

not, the centering procedure is easy to implement by removing their mean vectors from each data-point of them.

CCA finds two bases in the  $m_a$ - and  $m_b$ -dimensional spaces where  $\mathbf{x}^a$  and  $\mathbf{x}^b$  have the maximum correlation. More precisely, it first finds an  $m_a$ -dimensional projection vector  $\mathbf{u}_1$  and an  $m_b$ -dimensional projection vector  $\mathbf{v}_1$  such that the 1-dimensional projected signals  $\mathbf{u}_1^T \mathbf{x}^a$  and  $\mathbf{v}_1^T \mathbf{x}^b$  are maximally cross-correlated. Therefore, the aim of CCA is to find the maximum correlation coefficient  $\rho$  between these two projected signals

$$\rho(\mathbf{u}_1, \mathbf{v}_1) = \frac{\mathbf{u}_1^T \mathbf{R}_{ab} \mathbf{v}_1}{\sqrt{\mathbf{u}_1^T \mathbf{R}_{aa} \mathbf{u}_1 \cdot \mathbf{v}_1^T \mathbf{R}_{bb} \mathbf{v}_1}} \quad (1)$$

where  $\mathbf{R}_{ab} = E\{\mathbf{x}^a \mathbf{x}^{bT}\}$  is the cross-covariance matrix of  $\mathbf{x}^a$  and  $\mathbf{x}^b$ ,  $\mathbf{R}_{aa} = E\{\mathbf{x}^a \mathbf{x}^{aT}\}$  and  $\mathbf{R}_{bb} = E\{\mathbf{x}^b \mathbf{x}^{bT}\}$  are their auto-covariance matrices, with  $E\{\cdot\}$  representing the expectation operator.

Obtaining the maximum correlation coefficient can be characterized as an optimization problem that finds the projection vectors  $\mathbf{u}_1$  and  $\mathbf{v}_1$

$$\begin{cases} \max_{\mathbf{u}_1, \mathbf{v}_1} & \mathbf{u}_1^T \mathbf{R}_{ab} \mathbf{v}_1 \\ \text{s.t.} & \mathbf{u}_1^T \mathbf{R}_{aa} \mathbf{u}_1 = 1 \\ & \mathbf{v}_1^T \mathbf{R}_{bb} \mathbf{v}_1 = 1 \end{cases} \quad (2)$$

Next, CCA finds the projection vectors  $\mathbf{u}_2$  and  $\mathbf{v}_2$  such that the cross-correlation between  $\mathbf{u}_2^T \mathbf{x}^a$  and  $\mathbf{v}_2^T \mathbf{x}^b$  is maximized, whereas  $\mathbf{u}_2^T \mathbf{x}^a$  is uncorrelated with  $\mathbf{u}_1^T \mathbf{x}^a$ , and  $\mathbf{v}_2^T \mathbf{x}^b$  is uncorrelated with  $\mathbf{v}_1^T \mathbf{x}^b$ . A similar optimization problem can then be established as

$$\begin{cases} \max_{\mathbf{u}_2, \mathbf{v}_2} & \mathbf{u}_2^T \mathbf{R}_{ab} \mathbf{v}_2 \\ \text{s.t.} & \mathbf{u}_2^T \mathbf{R}_{aa} \mathbf{u}_2 = 1 \\ & \mathbf{u}_1^T \mathbf{R}_{aa} \mathbf{u}_2 = 0 \\ & \mathbf{v}_2^T \mathbf{R}_{bb} \mathbf{v}_2 = 1 \\ & \mathbf{v}_1^T \mathbf{R}_{bb} \mathbf{v}_2 = 0 \end{cases} \quad (3)$$

The subsequent projection vectors  $\mathbf{u}_j$  and  $\mathbf{v}_j$ , where  $j \leq \min(m_a, m_b)$ , can be found through the same way with additional constraints  $\mathbf{u}_i^T \mathbf{R}_{aa} \mathbf{u}_j = 0$  and  $\mathbf{v}_i^T \mathbf{R}_{bb} \mathbf{v}_j = 0$  for  $i=1, 2, \dots, j-1$ . It turns out that these projection vectors, as well as the corresponding canonical correlation coefficients, can be obtained by solving the following eigenvalue decomposition problem

$$\left( \mathbf{R}_{aa}^{-1} \mathbf{R}_{ab} \mathbf{R}_{bb}^{-1} \mathbf{R}_{ba} \right) \mathbf{u} = \rho^2 \mathbf{u} \quad (4)$$

$$\left( \mathbf{R}_{bb}^{-1} \mathbf{R}_{ba} \mathbf{R}_{aa}^{-1} \mathbf{R}_{ab} \right) \mathbf{v} = \rho^2 \mathbf{v} \tag{5}$$

where  $\mathbf{R}_{ba} = E\{\mathbf{x}^b \mathbf{x}^{aT}\} = \mathbf{R}_{ab}^T$ . The eigenvalues  $\rho^2$  are squared canonical correlation coefficients and the eigenvectors  $\mathbf{u}$  and  $\mathbf{v}$  are normalized canonical correlation basis vectors. Generally, only the non-zero solutions are of interest, and their number  $r$  is equal to the smaller of the dimensions of  $\mathbf{x}^a$  and  $\mathbf{x}^b$ , i.e.,  $r = \min(m_a, m_b)$ .

### 3. Establishment of sensor fault diagnosis method

To build a multivariate model, which considers and utilizes the dynamic or auto-regressive characteristics hidden in the health-monitoring data, CCA is introduced as a supervised dimensionality reduction technique. The sensor fault diagnosis method that mainly focuses on the fault detection and isolation objectives is then established.

#### 3.1 Dynamic characteristic in accelerometer measurement

Because the accelerometer measurement is always employed as an important part of vibration monitoring for civil infrastructures, it is a research objective in this paper. The dynamic characteristic, reflecting the correlations between the currently observed and future possible accelerometer responses, is an essential property of the monitored structure. Therefore, it should be considered in building the multivariate statistical model, based on which a fault diagnosis method can be established, of the structural accelerometer measurements to promote the fault diagnosis performance.

The auto-regressive model is a frequently applied technique that predicts the possible future response of a monitored structure based on the current measurements employing the dynamic characteristic. Given that  $\mathbf{x}(t) \in \mathfrak{R}^m$  denotes an accelerometer measurement at time  $t$ , the auto-regressive model can be mathematically represented as follows (Thanagasundram *et al.* 2008, Roy *et al.* 2015)

$$\mathbf{x}(t+1) = \sum_{i=1}^p \mathbf{A}_i \mathbf{x}(t-i+1) + \mathbf{e}(t+1) \tag{6}$$

where  $\mathbf{A}_i$  is the  $i$ th model coefficient matrix,  $\mathbf{x}(t+1)$  is the future response to be predicted,  $\mathbf{e}(t+1)$  is the model residual error and  $p$  is the model order that can be determined through the Akaike information criterion (Chiang *et al.* 2001).

#### 3.2 Dynamic modeling via canonical correlation analysis

When the dynamic characteristic is about building a correlation model between two multivariate observation datasets, the CCA technique is used for this purpose. This section proposes to employ CCA to build a multivariate statistical model, which considers the dynamic characteristic hidden in the accelerometer measurements, to develop an innovative sensor fault diagnosis method with applications to SHM.

To model the dynamic characteristic hidden in the structural accelerometer measurements via CCA, the current and future observation vectors  $\mathbf{x}^c$  and  $\mathbf{x}^f$  at time  $t$  are first defined as follows

$$\mathbf{x}^c(t) = [\mathbf{x}^T(t), \mathbf{x}^T(t-1), \dots, \mathbf{x}^T(t-p+1)]^T \in \mathfrak{R}^{mp} \quad (7)$$

$$\mathbf{x}^f(t) = \mathbf{x}(t+1) \in \mathfrak{R}^m \quad (8)$$

where  $p$  is the auto-regressive model order. The current and future observation datasets can then be assembled from the fault-free training dataset.

A data pre-whitening procedure could be implemented for the current and future observation datasets to simplify the CCA computational process shown in Eq. 4 and Eq. 5 (Karhunen *et al.* 2013). The pre-whitening procedure for the current and future observation vectors is mathematically represented as follows:

$$\tilde{\mathbf{x}}^c(t) = \mathbf{Q}^c \mathbf{x}^c(t) \quad (9)$$

$$\tilde{\mathbf{x}}^f(t) = \mathbf{Q}^f \mathbf{x}^f(t) \quad (10)$$

where  $\tilde{\mathbf{x}}^c(t)$  and  $\tilde{\mathbf{x}}^f(t)$  are the whitened data-points of the current and future observation vectors, respectively,  $\mathbf{Q}^c$  and  $\mathbf{Q}^f$  are the corresponding whitening matrices.

To calculate the whitening matrices  $\mathbf{Q}^c$  and  $\mathbf{Q}^f$ , the principal component analysis technique is always utilized to model the datasets to be whitened:

$$\mathbf{R}_{cc} = E\{\mathbf{x}^c \mathbf{x}^{cT}\} = \mathbf{P}^c \mathbf{A}^c \mathbf{P}^{cT} \quad (11)$$

$$\mathbf{R}_{ff} = E\{\mathbf{x}^f \mathbf{x}^{fT}\} = \mathbf{P}^f \mathbf{A}^f \mathbf{P}^{fT} \quad (12)$$

where  $\mathbf{R}_{cc}$  and  $\mathbf{R}_{ff}$  are the auto-covariance matrices of the current and future observation datasets, respectively,  $\mathbf{P}^c$  and  $\mathbf{P}^f$  are the transformation matrices of principal component analysis,  $\mathbf{A}^c$  and  $\mathbf{A}^f$  are the diagonal matrices that contain the variances of the principal components in descending order. The whitening matrices can then be represented as

$$\mathbf{Q}^c = (\mathbf{A}^c)^{-1/2} \mathbf{P}^{cT} \quad (13)$$

$$\mathbf{Q}^f = (\mathbf{A}^f)^{-1/2} \mathbf{P}^{fT} \quad (14)$$

After the pre-whitening procedure, any two variables in the pre-whitened dataset are statistically uncorrelated.

The CCA technique is then applied to model the correlations between the current and future observation datasets which are pre-whitened

$$(\widehat{\mathbf{R}}_{cc}^{-1} \widehat{\mathbf{R}}_{cf} \widehat{\mathbf{R}}_{ff}^{-1} \widehat{\mathbf{R}}_{fc}) \mathbf{u} = \rho^2 \mathbf{u} \quad (15)$$

$$(\widehat{\mathbf{R}}_{ff}^{-1} \widehat{\mathbf{R}}_{fc} \widehat{\mathbf{R}}_{cc}^{-1} \widehat{\mathbf{R}}_{cf}) \mathbf{v} = \rho^2 \mathbf{v} \quad (16)$$

where  $\widehat{\mathbf{R}}_{cc} = E\{\widehat{\mathbf{x}}^c \widehat{\mathbf{x}}^{cT}\}$  and  $\widehat{\mathbf{R}}_{ff} = E\{\widehat{\mathbf{x}}^f \widehat{\mathbf{x}}^{fT}\}$  are the auto-covariance matrices of the current and future observation datasets, respectively, after being pre-whitened,  $\widehat{\mathbf{R}}_{cf} = E\{\widehat{\mathbf{x}}^c \widehat{\mathbf{x}}^{fT}\}$  is the cross-covariance matrix of  $\widehat{\mathbf{x}}^c$  and  $\widehat{\mathbf{x}}^f$  with  $\widehat{\mathbf{R}}_{fc} = E\{\widehat{\mathbf{x}}^f \widehat{\mathbf{x}}^{cT}\} = \widehat{\mathbf{R}}_{cf}^T$ .

The auto-covariance matrices corresponding to the pre-whitened current and future observation datasets are actually two identity matrices, i.e.,  $\widehat{\mathbf{R}}_{cc} = \mathbf{I}_{mp}$  and  $\widehat{\mathbf{R}}_{ff} = \mathbf{I}_m$ . Considering that  $\widehat{\mathbf{R}}_{fc} = \widehat{\mathbf{R}}_{cf}^T$ , the CCA computational process shown in Eqs. (15) and (16) is then simplified as follows

$$(\widehat{\mathbf{R}}_{cf} \widehat{\mathbf{R}}_{cf}^T) \mathbf{u} = \rho^2 \mathbf{u} \quad (17)$$

$$(\widehat{\mathbf{R}}_{fc} \widehat{\mathbf{R}}_{fc}^T) \mathbf{v} = \rho^2 \mathbf{v} \quad (18)$$

The eigenvalue decomposition problem shown in Eqs. (17) and (18) could be further reduced to a singular-value decomposition problem as follows

$$\widehat{\mathbf{R}}_{cf} = E\{\widehat{\mathbf{x}}^c \widehat{\mathbf{x}}^{fT}\} = \mathbf{U} \boldsymbol{\Sigma} \mathbf{V}^T \quad (19)$$

where  $\mathbf{U} = [\mathbf{u}_1, \mathbf{u}_2, \dots, \mathbf{u}_{mp}] \in \mathfrak{R}^{mp \times mp}$  is a matrix consisting of all the left singular vectors,  $\mathbf{V} = [\mathbf{v}_1, \mathbf{v}_2, \dots, \mathbf{v}_m] \in \mathfrak{R}^{m \times m}$  is a matrix consisting of all the right singular vectors, and  $\boldsymbol{\Sigma} = [\tilde{\boldsymbol{\Sigma}} | \mathbf{0}]^T \in \mathfrak{R}^{mp \times m}$  is the singular-value matrix with  $\tilde{\boldsymbol{\Sigma}} = \text{diag}(\rho_1, \rho_2, \dots, \rho_m)$  a diagonal matrix and  $\mathbf{0} \in \mathfrak{R}^{m \times m(p-1)}$  a zero-matrix.

The canonical correlation variables  $\mathbf{z}$  and  $\mathbf{r}$ , which respectively correspond to the current and future observation vectors, could then be generated as follows

$$\mathbf{z}(t) = \mathbf{U}^T \widehat{\mathbf{x}}^c(t) = \mathbf{U}^T \mathbf{Q}^c \mathbf{x}^c(t) = \mathbf{J} \mathbf{x}^c(t) \quad (20)$$

$$\mathbf{r}(t) = \mathbf{V}^T \widehat{\mathbf{x}}^f(t) = \mathbf{V}^T \mathbf{Q}^f \mathbf{x}^f(t) = \mathbf{L} \mathbf{x}^f(t) \quad (21)$$

where  $\mathbf{J}$  and  $\mathbf{L}$  are the canonical correlation generative matrices corresponding to the current and future observation vectors, respectively. They are mathematically represented as

$$\mathbf{J} = \mathbf{U}^T \mathbf{Q}^c \quad (22)$$

$$\mathbf{L} = \mathbf{V}^T \mathbf{Q}^f \quad (23)$$

Through the above two matrices, the canonical correlation variables could be calculated expediently. Every two components of these canonical correlation variables are also statistically uncorrelated for the following reasons

$$\mathbf{R}_{zz} = E\{\mathbf{z} \mathbf{z}^T\} = \mathbf{U}^T E\{\widehat{\mathbf{x}}^c \widehat{\mathbf{x}}^{cT}\} \mathbf{U} = \mathbf{I}_{mp} \quad (24)$$

$$\mathbf{R}_{rr} = E\{\mathbf{r} \mathbf{r}^T\} = \mathbf{V}^T E\{\widehat{\mathbf{x}}^f \widehat{\mathbf{x}}^{fT}\} \mathbf{V} = \mathbf{I}_m \quad (25)$$

### 3.3 Fault detection scheme

This section, based on the CCA model built through analyzing the fault-free measurement data, defines two fault detection statistics to monitor the quality of the current sensor output data and to detect the corresponding sensor faults. The current observation vector defined in the previous section is chosen to accomplish this purpose.

The first  $m$  components of the canonical correlation variable  $\mathbf{z}$  are defined as the systematic part that is closely correlated with the future observation vector and assembled into a column vector  $\mathbf{z}_s$ , as well as the others are defined as the noisy part and assembled into a column vector  $\mathbf{z}_n$ . Therefore, the canonical correlation variable  $\mathbf{z}$  could be represented as the following block form at time  $t$

$$\mathbf{z}(t) = \begin{bmatrix} \mathbf{z}_s^T(t) \\ \mathbf{z}_n^T(t) \end{bmatrix}^T \quad (26)$$

The generative process of the canonical correlation variable  $\mathbf{z}$  could also be mathematically represented as the following block form

$$\mathbf{z}(t) = \begin{bmatrix} \mathbf{z}_s(t) \\ \mathbf{z}_n(t) \end{bmatrix} = \begin{bmatrix} \mathbf{J}_s \\ \mathbf{J}_n \end{bmatrix} \mathbf{x}^c(t) \quad (27)$$

or

$$\mathbf{z}_s(t) = \mathbf{J}_s \mathbf{x}^c(t) \quad (28)$$

$$\mathbf{z}_n(t) = \mathbf{J}_n \mathbf{x}^c(t) \quad (29)$$

where  $\mathbf{J}_s$  is called the system generative matrix which contains the first  $m$  rows of  $\mathbf{J}$ , and  $\mathbf{J}_n$  is called the noise generative matrix which contains the last  $m(p-1)$  rows of  $\mathbf{J}$ .

The fault detection statistic for the systematic canonical correlation variable, i.e., the  $T_s^2$  statistic, is defined as

$$T_s^2 = \mathbf{z}_s^T \mathbf{z}_s = \mathbf{x}^{cT} (\mathbf{J}_s^T \mathbf{J}_s) \mathbf{x}^c \quad (30)$$

If the health-monitoring data follows a Gaussian distribution, the control limit (or called the threshold) for  $T_s^2$  could be calculated through the following  $F$ -distribution (Antoine and Çlinar 1997)

$$T_{s,\text{lim}}^2(\alpha) \approx \frac{m(m^2 p^2 - 1)}{mp(mp - m)} F_{m, mp-m}(\alpha) \quad (31)$$

where  $\alpha$  is called the significance level, this parameter is generally set to a pinging value, e.g., 0.01.

The fault detection statistic for the noisy canonical correlation variable, i.e., the  $T_n^2$  statistic, could be similarly defined as follows

$$T_n^2 = \mathbf{z}_n^T \mathbf{z}_n = \mathbf{x}^{cT} (\mathbf{J}_n^T \mathbf{J}_n) \mathbf{x}^c \tag{32}$$

If the health-monitoring data has a Gaussian distribution, the control limit for  $T_n^2$  could also be calculated via the  $F$ -distribution as follows

$$T_{n,\text{lim}}^2(\alpha) \approx \frac{m(p-1)(m^2 p^2 - 1)}{m^2 p} F_{mp-m,m}(\alpha) \tag{33}$$

When the health-monitoring is not Gaussian distributed, the kernel density estimation (KDE) technique (Chen *et al.* 2000) could be employed to estimate the probabilistic distribution and then to calculate the control limits for both  $T_s^2$  and  $T_n^2$  statistics. In this paper, the KDE technique is used to compute the control limits as it can handle both Gaussian and non-Gaussian distributions.

### 3.4 Fault isolation scheme

After a fault is detected to occur in the sensor network, fault isolation procedure should be implemented to identify the specific faulty sensor. This section, through the contribution analysis methodology (Qin 2003), proposes two fault isolation indices that can be used to identify the faulty sensor among the sensor network.

Eqs. (30) and (32) could be further represented in the following forms

$$T_s^2 = \mathbf{x}^{cT} (\mathbf{J}_s^T \mathbf{J}_s) \mathbf{x}^c = \mathbf{x}^{cT} \Phi_s \mathbf{x}^c \tag{34}$$

$$T_n^2 = \mathbf{x}^{cT} (\mathbf{J}_n^T \mathbf{J}_n) \mathbf{x}^c = \mathbf{x}^{cT} \Phi_n \mathbf{x}^c \tag{35}$$

where  $\Phi_s \in \mathfrak{R}^{mp \times mp}$  and  $\Phi_n \in \mathfrak{R}^{mp \times mp}$  are matrices corresponding to the system and noise generative matrices, respectively. Their definitions are used to derivate the contribution analysis based fault isolation indices

$$\Phi_s = \mathbf{J}_s^T \mathbf{J}_s \tag{36}$$

$$\Phi_n = \mathbf{J}_n^T \mathbf{J}_n \tag{37}$$

According to Eqs. (34) and (35), the  $T_s^2$  and  $T_n^2$  statistics could be further decomposed into the following summation type

$$T_s^2 = \mathbf{x}^{cT} \cdot \sum_{i=1}^{mp} x_i^c \phi_{s,i} = \sum_{i=1}^{mp} x_i^c \cdot \phi_{s,i}^T \mathbf{x}^c \tag{38}$$

$$T_n^2 = \mathbf{x}^{cT} \cdot \sum_{i=1}^{mp} x_i^c \phi_{n,i} = \sum_{i=1}^{mp} x_i^c \cdot \phi_{n,i}^T \mathbf{x}^c \tag{39}$$

where  $\phi_{s,i} \in \mathfrak{R}^{mp}$  and  $\phi_{n,i} \in \mathfrak{R}^{mp}$  are the  $i$ th columns of  $\Phi_s$  and  $\Phi_n$ , respectively.

Therefore, the contributions of the  $i$ th variable in the current observation vector  $\mathbf{x}^c$  to the  $T_s^2$  and  $T_n^2$  statistics can be defined as  $\text{cont}_{s,i}$  and  $\text{cont}_{n,i}$ , respectively, and are given as

follows

$$\text{cont}_{s,i} = x_i^c \cdot \phi_{s,i}^T \mathbf{x}^c \tag{40}$$

$$\text{cont}_{n,i} = x_i^c \cdot \phi_{n,i}^T \mathbf{x}^c \tag{41}$$

The fault isolation indices corresponding to the  $T_s^2$  and  $T_n^2$  statistics are defined as follows

$$\text{CONT}_{s,j} = \sum_{k=1}^p \text{cont}_{s,j+m(k-1)} = \sum_{k=1}^p x_{j+m(k-1)}^c \cdot \phi_{s,j+m(k-1)}^T \mathbf{x}^c \tag{42}$$

$$\text{CONT}_{n,j} = \sum_{k=1}^p \text{cont}_{n,j+m(k-1)} = \sum_{k=1}^p x_{j+m(k-1)}^c \cdot \phi_{n,j+m(k-1)}^T \mathbf{x}^c \tag{43}$$

When the value of the fault isolation indices  $\text{CONT}_{s,j}$  and  $\text{CONT}_{n,j}$  corresponding to a specific sensor reaches the maximum, the faulty sensor is isolated through the indices.

#### 4. Sensor fault diagnosis procedure

The proposed sensor fault diagnosis method consists of two sub-procedures, that is the fault detection sub-procedure and the fault isolation sub-procedure. This section describes the implementation processes of these two sub-procedures in detail.

##### 4.1 Fault detection sub-procedure

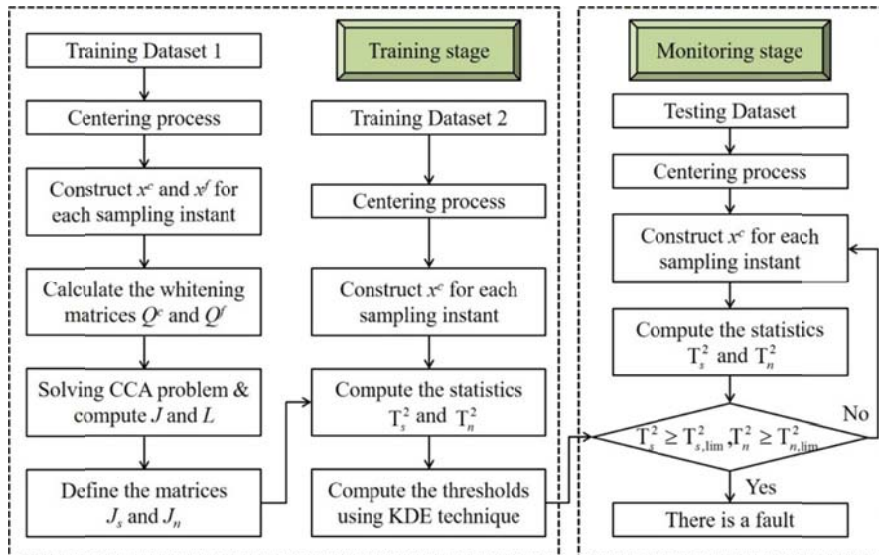


Fig. 1 Flowchart of the fault detection sub-procedure

Three datasets are used for the fault detection sub-procedure, i.e., Training Dataset 1, Training Dataset 2 and the Testing Dataset. Training Datasets 1 and 2 are used for the training stage whereas the Testing Dataset is used for the monitoring stage. A flowchart of the fault detection sub-procedure is shown in Fig. 1. And the detailed implementation process is illustrated as follows:

Training stage using Training Dataset 1:

Step 1: Calculate the mean vector of Training Dataset 1 and then center this dataset by removing the mean vector from all data-points.

Step 2: Construct the current and future observation vectors  $\mathbf{x}^c$  and  $\mathbf{x}^f$ , respectively, at each time instant using Eq. (7) and Eq. (8), and then assemble the corresponding current and future observation datasets.

Step 3: Calculate the whitening matrices  $\mathbf{Q}^c$  and  $\mathbf{Q}^f$  for the current and future observation vectors, respectively, using Eqs. (13) and (14).

Step 4: Solve the CCA problem shown in Eq. (19) using the singular-value decomposition technique, and compute the canonical correlation generative matrices  $\mathbf{J}$  and  $\mathbf{L}$ , respectively, using Eqs. (22) and (23).

Step 5: Define the first  $m$  rows of  $\mathbf{J}$  as the system generative matrix  $\mathbf{J}_s$ , define the last  $m(p-1)$  rows of  $\mathbf{J}$  as the noise generative matrix  $\mathbf{J}_n$ , and preserve  $\mathbf{J}_s$  and  $\mathbf{J}_n$  for the subsequent fault detection and isolation stages.

Training stage using Training Dataset 2:

Step 1: Center Training Dataset 2 by removing the mean vector of Training Dataset 1 from all data-points.

Step 2: Construct the current observation vector  $\mathbf{x}^c$  at each time instant using Eq. (7).

Step 3: Compute the two fault detection statistics  $T_s^2$  and  $T_n^2$  defined in Eqs. (30) and (32) for the current observation vector  $\mathbf{x}^c$  constructed in Step 2.

Step 4: Compute and preserve the thresholds for both the  $T_s^2$  and  $T_n^2$  statistics using the KDE technique after the  $T_s^2$  and  $T_n^2$  statistics for all of the current observation vectors are computed.

Monitoring stage using the Testing Dataset:

Step 1: Center the Testing Dataset by removing the mean vector of Training Dataset 1 from all data-points.

Step 2: Construct the current observation vector  $\mathbf{x}^c$  at the current monitoring time instant using Eq. (7).

Step 3: Compute the two fault detection statistics  $T_s^2$  and  $T_n^2$  defined in Eqs. (30) and (32) for the current observation vector  $\mathbf{x}^c$  constructed in Step 2.

Step 4: Decide whether there is a fault occurred in the sensor network by judging if the  $T_s^2$  or  $T_n^2$  statistic exceeds their corresponding thresholds: go to the fault isolation sub-procedure if there is a fault or back to step 2 and continue to monitor the next current observation vector if there is

not.

#### 4.2 Fault isolation sub-procedure

The fault isolation sub-procedure is used to identify the specific faulty sensor after a fault is detected in the sensor network. Only the Testing Dataset is used for the fault isolation sub-procedure. The  $j$ th sensor is identified as the faulty sensor if its corresponding fault isolation index  $CONT_{s,j}$  or  $CONT_{n,j}$ , computed from Eqs. (42) and (43), obtains the largest value.

### 5. Case studies

To validate the effectiveness and capability of the new proposed sensor fault diagnosis method, case studies using the benchmark model developed by the University of Central Florida for bridge health monitoring (Catbas *et al.* 2008) are considered in this section. This benchmark model has been widely used for demonstrating various algorithms in different structural health monitoring aspects, e.g., damage identification and finite-element model updating (Gul and Catbas 2011, Erdogan *et al.* 2014).

The physical structure of the benchmark model is a steel grid of which the girders and support columns are constructed using steel sections  $S3 \times 5.7$  and  $W12 \times 26$ , respectively. The three-dimensional view of this benchmark structure is shown in Fig. 2(a), it is seen that there are totally two spans and six support columns in the structure. The corresponding plan view of the steel girders is shown in Fig. 2(b) which gives the detailed size.

The finite-element model of this benchmark structure consists of 182 elements and 177 nodes and was created as a MATLAB (The Mathworks 2014) toolbox by the developer. This makes it very convenient for the researchers to generate health-monitoring data. A number of damage cases with different levels can be simulated with the associated numerical benchmark model. Various sensors, such as accelerometers, displacement gages and strain gages, could be placed on the model to collect static and dynamic responses.

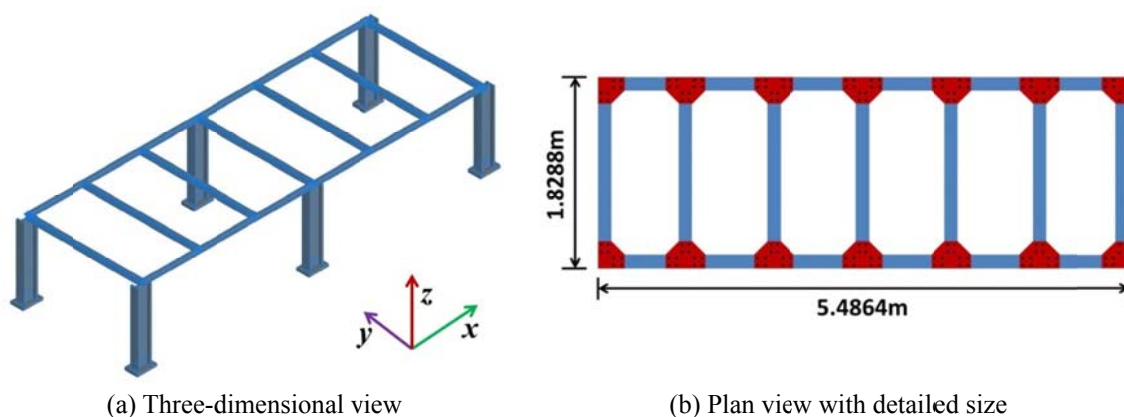


Fig. 2 Diagram of the benchmark structure (adapted from Catbas *et al.* 2008)

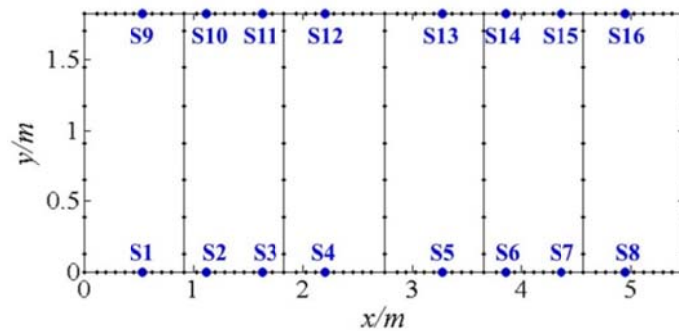


Fig. 3 Sensor location on the finite-element model of the benchmark structure; the symbol S# represents sensor #

Table 1 Corresponding relationship of the sensor and finite-element node number

Sensor number	Node number	Sensor number	Node number
1	63	9	105
2	66	10	108
3	72	11	114
4	75	12	117
5	84	13	126
6	87	14	129
7	93	15	135
8	96	16	138

The acceleration responses, at different locations of the numerical benchmark model, under random excitations were first simulated. Meanwhile, the responses with additional Gaussian noises were employed in this section as sensor output data. For the choice of the noise level, the signal-to-noise-ratio was set to as low as 20dB. Notice that only the vertical acceleration measurements were used for the purpose of validation and no accelerometer was placed at the support nodes because their vertical accelerations were almost zero. There were totally 16 accelerometers installed on the structure and the sensor location on the finite-element model of the benchmark structure can be seen in Fig. 3. The sensor placement information for this benchmark model is shown in Table 1, where the corresponding relationship of the sensor and finite-element node number is given in detail.

Three datasets, i.e., Training Dataset 1, Training Dataset 2 and the Testing Dataset, were generated through the numerical benchmark model. Training Datasets 1 and 2 were fault-free monitoring datasets, and both lasted for 40 seconds. The Testing Dataset lasted for 80 seconds, of which the first 40 seconds consisted of normal data, and the last 40 seconds used for simulating faulty data.

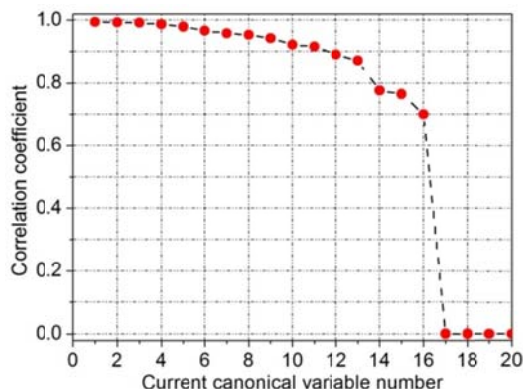


Fig. 4 Correlation coefficients of the canonical correlation variables of the current observation vectors with those of the future ones

Table 2 Mathematical representation of the bias and gain modes of sensor fault

Fault type	Mathematical representation
Bias	$x_f(t) = x(t) + B \cdot \sigma + \eta(t)$
Gain	$x_f(t) = (1 + G) \cdot [x(t) + \eta(t)]$

Training Dataset 1 was used to build the CCA model and then to compute the canonical correlation generative matrices. Fig. 4 shows the correlation coefficients of the canonical correlation variables of the current observation vectors with those of the future ones. It can be seen that only the first 16 canonical correlation coefficients are non-zero (notice that only the first 20 canonical correlation coefficients are plotted on the figure as the remaining values still equal zero), which means that the first 16 column vectors of the canonical correlation generative matrix corresponding to the current observation vectors are used to form the system generative matrix and that the remaining are used to form the noise generative matrix.

Training Dataset 2 was used to compute the control limit values via the KDE technique. The Testing Dataset was then used to validate the capability of the proposed CCA based sensor fault diagnosis method.

There are two types of sensor fault modes, i.e., the bias and gain sensor fault modes, which are the typical modes of the additive and multiplicative sensor faults (Abdelghani and Friswell 2004, Abdelghani and Friswell 2007, Kullaa 2010), respectively. Both of these were considered in this section. Table 2 summarized the mathematical representation of these two sensor fault modes. The variable  $x_f(t)$  represents the faulty sensor output,  $x(t)$  is the nominal sensor measurement,  $\eta(t)$  is the measurement noise, and  $\sigma$  represents the standard deviation of the term  $x(t) + \eta(t)$ . The terms  $B$  and  $G$  controls the magnitudes of the bias and gain faults, respectively. For fault simulation, the relatively small magnitudes of the bias and gain faults were chosen, e.g.,  $B=0.5$  and  $G=0.5$ , to show the superiority of the proposed method.

5.1 Diagnostic results for bias fault

Sensors 1-8 were considered in turn as the research objects for the purpose of validation in this section. A fault case, where a bias fault occurred in each of the aforementioned 8 sensors with  $B=0.5$  from 40 s to 80 s, was simulated.

The receiver operating characteristic (ROC) curve technique (Lu *et al.* 2009) was used to evaluate and compare the fault detection performances of the two proposed fault detection statistics with the traditional principal component analysis (PCA)-based statistics (Qin 2003, Yin *et al.* 2012), as well as the dynamic principal component analysis (DPCA)-based statistics (Ku *et al.* 1995).

Generally, the area under the ROC curve (AUC) is applied to quantify the fault detection performance of a statistic. The AUC value of an arbitrary fault detection statistic ranges from 0.5 to 1.0. When the AUC value equals 0.5, the fault detection performance of this statistic becomes the worst, i.e., the statistic is a random detector. When the AUC value equals 1.0, the fault detection performance of this statistic becomes the best, i.e., the statistic is a perfect detector.

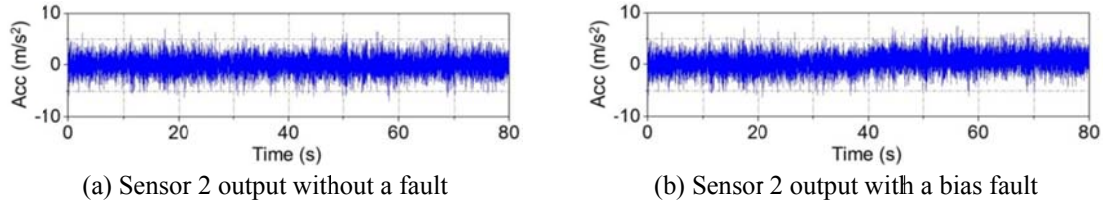
Table 3 shows the AUC values of the PCA-, DPCA- and CCA-based fault detection statistics for the bias fault case. The AUC values of the PCA- and DPCA-based statistics are just above 0.5, indicating that their fault detection performances are very poor. The AUC values of the CCA-based statistics, however, are very close to 1.0, indicating that the fault detection performances of the new proposed statistics are nearly perfect and preferable to the PCA- and DPCA-based ones.

As a special example, the bias fault occurring in sensor 2 was studied in detail. Fig. 5(a) shows the fault-free waveform graph of sensor 2, whereas Fig. 5(b) shows the faulty sensor output with  $B=0.5$ .

The fault detection results of the PCA- and DPCA-based  $T^2$  and SPE statistics are shown in Fig. 6. The fault detection rates of these four statistics are 1.50%, 1.15%, 1.37% and 4.08%. This also demonstrates that their fault detection abilities are quite inferior.

Table 3 Comparison of AUC values for the PCA-, DPCA- and CCA-based methods (Bias fault case)

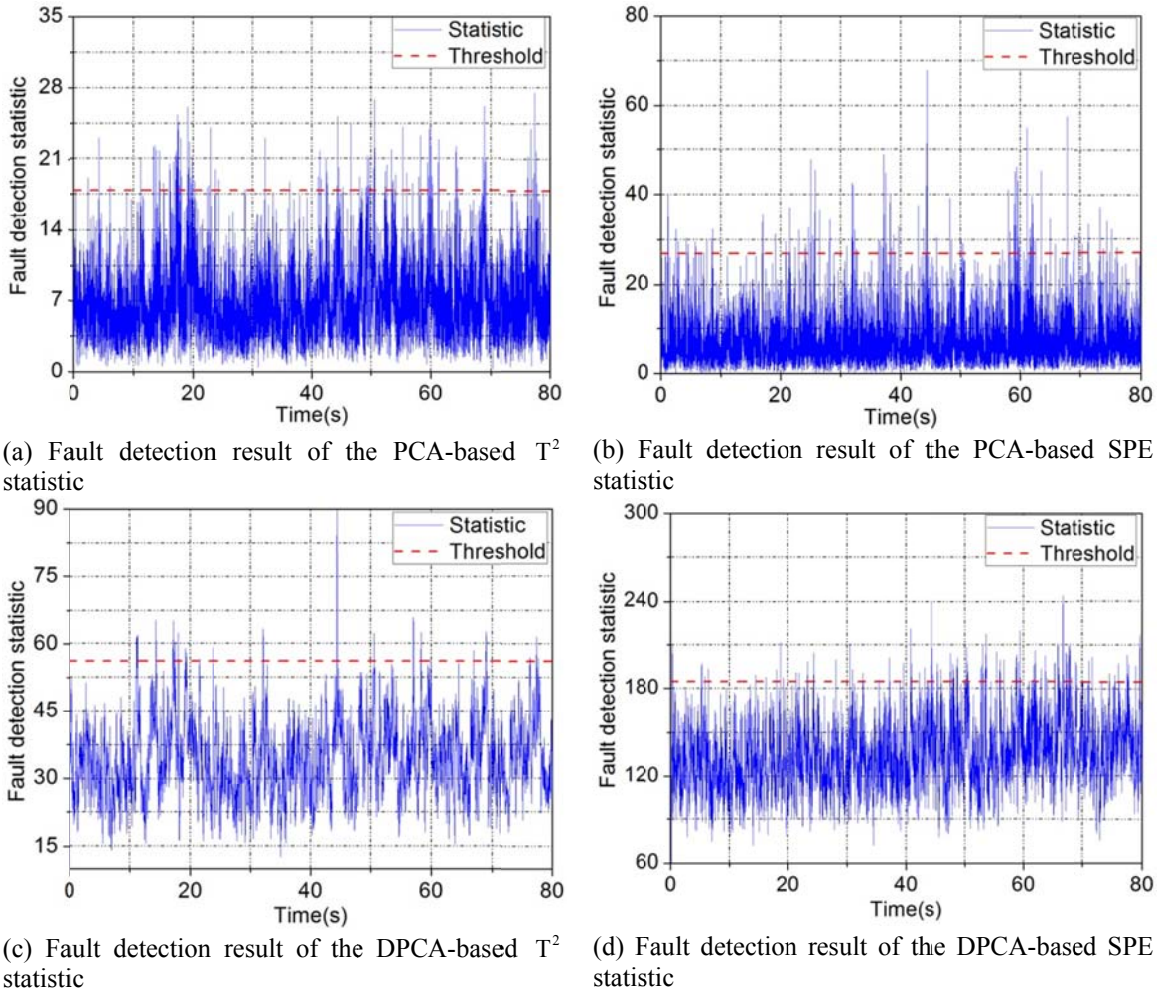
Sensor #	PCA based method		DPCA based method		CCA based method	
	$T^2$	SPE	$T^2$	SPE	$T_s^2$	$T_n^2$
1	0.5662	0.5338	0.5843	0.6637	<b>0.9954</b>	<b>0.9956</b>
2	0.5643	0.5338	0.5810	0.6539	<b>0.9954</b>	<b>0.9956</b>
3	0.5635	0.5346	0.5875	0.6188	<b>0.9954</b>	<b>0.9956</b>
4	0.5634	0.5398	0.5811	0.6520	<b>0.9954</b>	<b>0.9956</b>
5	0.5635	0.5403	0.5808	0.6539	<b>0.9954</b>	<b>0.9956</b>
6	0.5636	0.5353	0.5878	0.6168	<b>0.9954</b>	<b>0.9956</b>
7	0.5646	0.5328	0.5809	0.6503	<b>0.9954</b>	<b>0.9956</b>
8	0.5660	0.5347	0.5839	0.6608	<b>0.9954</b>	<b>0.9956</b>



(a) Sensor 2 output without a fault

(b) Sensor 2 output with a bias fault

Fig. 5 Sensor 2 output of the testing data without or with a bias fault



(a) Fault detection result of the PCA-based  $T^2$  statistic

(b) Fault detection result of the PCA-based SPE statistic

(c) Fault detection result of the DPCA-based  $T^2$  statistic

(d) Fault detection result of the DPCA-based SPE statistic

Fig. 6 Fault detection results of the PCA- and DPCA-based statistics for the bias fault case

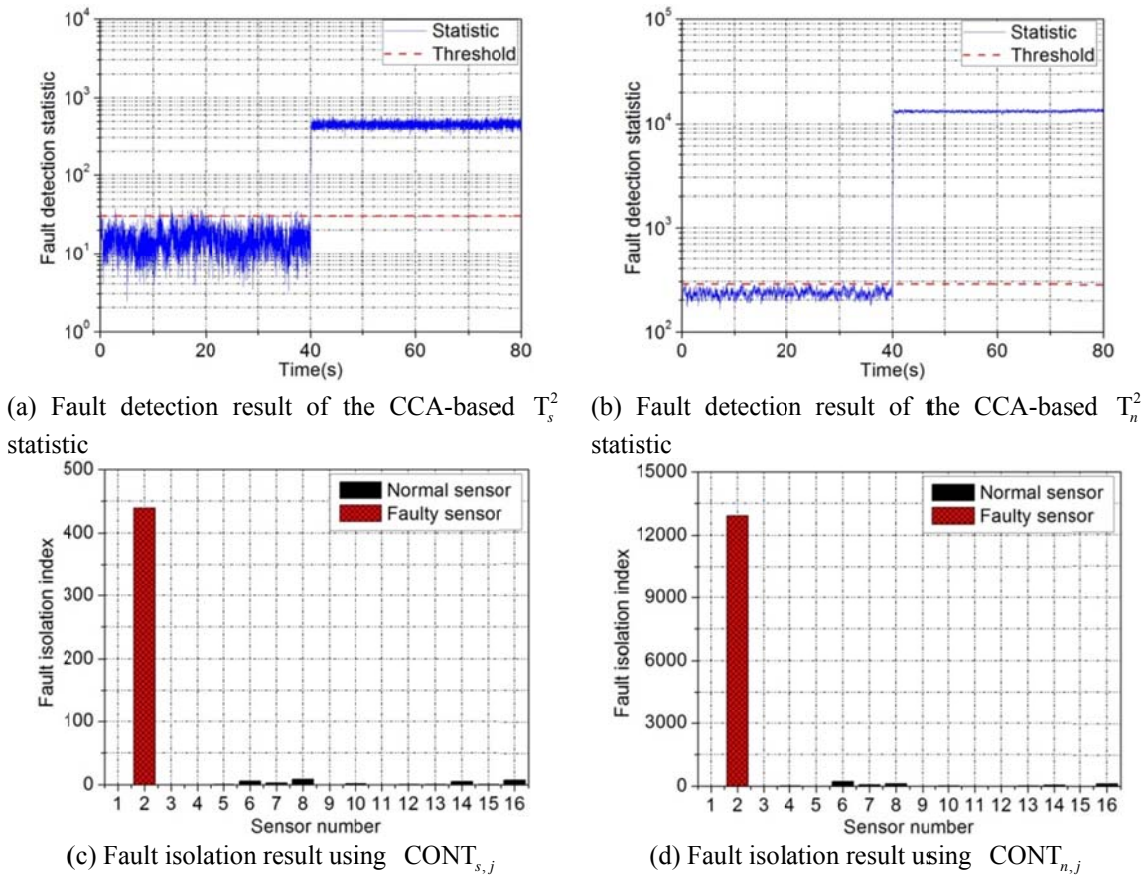


Fig. 7 Fault diagnosis results of the proposed CCA-based method for the bias fault case

The fault diagnosis results of the proposed CCA-based method are shown in Fig. 7. The fault detection results of the CCA-based  $T_s^2$  and  $T_n^2$  statistics are shown in Figs. 7(a) and 7(b), respectively. The fault detection rates of these two statistics are both 100%, which demonstrates that their fault detection performances are almost perfect. The fault isolation results of both  $CONT_{s,j}$  and  $CONT_{n,j}$ , which are shown in Figs. 7(c) and 7(d) respectively, indicate that the faulty sensor is successfully identified as sensor 2.

### 5.2 Diagnostic results for gain fault

The same with section 5.1, sensors 1-8 were still considered for the purpose of validation in this section. A fault case, with a gain fault occurred in each of the aforementioned 8 sensors with  $G=0.5$  from 40 s to 80 s, was simulated.

Table 4 shows the AUC values of the PCA-, DPCA- and CCA-based fault detection statistics for the gain fault case. The AUC values of the PCA-based statistics are just above 0.5, which indicates that their fault detection performances are very poor. The AUC values of the DPCA-based statistics exceed 0.6 or 0.7, which indicates that the fault detection performances

obtain a small increase when the dynamic characteristic is considered but are still not excellent. However, the AUC values of the CCA-based statistics are very close to 1.0. This indicates that the fault detection performances of the new proposed statistics are nearly perfect and preferable to the PCA- and DPCA-based statistics.

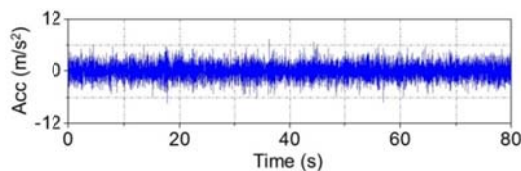
As a special example, the gain fault that occurred in sensor 6 is studied in detail. Fig. 8(a) shows the fault-free waveform graph of sensor 6, whereas Fig. 8(b) shows the faulty sensor output with  $G=0.5$ .

The fault detection results of the PCA- and DPCA-based  $T^2$  and SPE statistics are shown in Fig. 9. The fault detection rates of these four statistics are respectively 2.30%, 1.68%, 3.54% and 7.73%, demonstrating that their fault detection abilities are quite inferior.

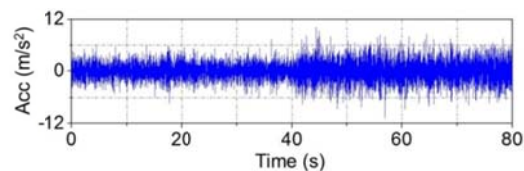
The fault diagnosis results of the proposed CCA-based method are shown in Fig. 10. The fault detection results of the CCA-based  $T_s^2$  and  $T_n^2$  statistics are respectively shown in Figs. 10(a) and 10(b). The fault detection rates of these two statistics are 92.36% and 99.98%, respectively. This also demonstrates that their fault detection performances are nearly perfect. The fault isolation results of  $CONT_{s,j}$  and  $CONT_{n,j}$ , which are shown in Figs. 10(c) and 10(d) respectively, indicate that the faulty sensor is successfully identified as sensor 6.

Table 4 Comparison of AUC values for PCA-, DPCA- and CCA-based methods (Gain fault cases)

Sensor #	PCA based method		DPCA based method		CCA based method	
	$T^2$	SPE	$T^2$	SPE	$T_s^2$	$T_n^2$
1	0.5990	0.5450	0.6513	0.7011	<b>0.9691</b>	<b>0.9955</b>
2	0.5905	0.5561	0.6639	0.7110	<b>0.9887</b>	<b>0.9956</b>
3	0.5860	0.5498	0.6638	0.6840	<b>0.9856</b>	<b>0.9955</b>
4	0.5866	0.5590	0.6275	0.7062	<b>0.9637</b>	<b>0.9956</b>
5	0.5874	0.5571	0.6297	0.7079	<b>0.9713</b>	<b>0.9956</b>
6	0.5873	0.5500	0.6634	0.6936	<b>0.9850</b>	<b>0.9954</b>
7	0.5924	0.5527	0.6622	0.7096	<b>0.9877</b>	<b>0.9956</b>
8	0.5979	0.5438	0.6499	0.7070	<b>0.9840</b>	<b>0.9955</b>



(a) Sensor 6 output without a fault



(b) Sensor 6 output with a gain fault

Fig. 8 Sensor 6 output of the testing data without or with a gain fault

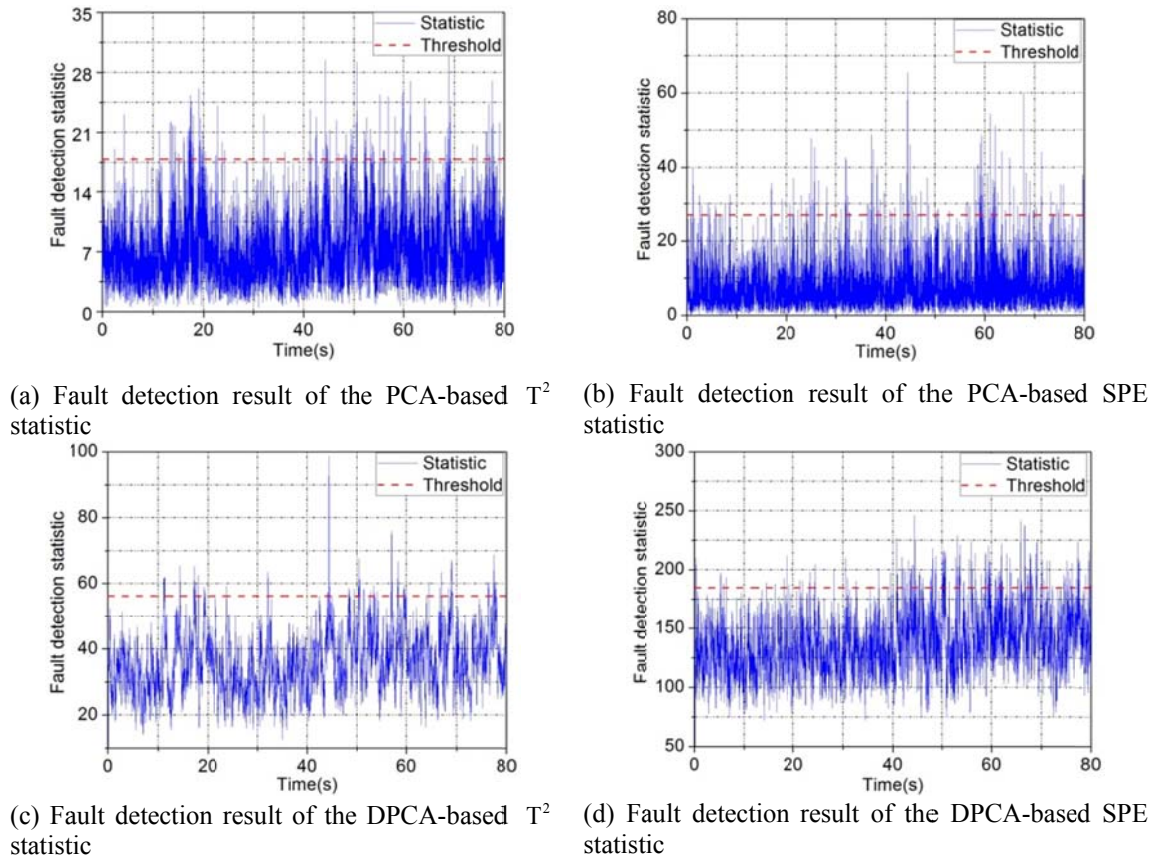


Fig. 9 Fault detection results of the PCA- and DPCA-based statistics for the gain fault case

## 6. Conclusions

Diagnosing various types of sensor fault prior to the application of any SHM algorithm is of great significance as it avoids false health evaluation results for the monitored infrastructures and reduces unnecessary maintenance costs due to false alarms. However, the sensor fault diagnosis technology has not received the attention that it deserves in the SHM field. This paper proposed an innovative sensor fault diagnosis method based on the CCA technique. The investigations carried out in this paper indicated the following conclusions:

(1) The dynamic behaviors hidden in the health-monitoring data were characterized by the auto-regressive model that predicted the future data-points through the current observed data-points. Hence, a statistical correlation property existed between the future and the current observation data-points. The CCA technique was suitably used to build a multivariate statistical model to characterize the correlations the current and future observation data-points. Based on this, a sensor fault diagnosis method that considered the dynamic or auto-regressive characteristics was established.

(2) Solving the above CCA model provided two generative matrices, i.e., the current and the future canonical correlation generative matrices. The current canonical correlation generative

matrix was used to establish the sensor fault diagnosis method. This matrix was then divided into two sub-matrices consisting of the systematic and the noisy parts of the generative matrix, according to the size of the canonical correlation coefficients. The fault detection purpose of the sensor network was realized through the definition of two statistics corresponding to the system and the noise generative matrices. The faulty sensor identification objective was achieved by the derivation of two fault isolation indices through using the contribution analysis methodology.

(3) Case studies were carried out to validate and demonstrate the efficacy of the new proposed sensor fault diagnosis method using the benchmark structure developed by the University of Central Florida for bridge health monitoring. The ROC curve was then employed as a standard technique to compare the fault detection performances of the PCA-based, the DPCA-based and the CCA-based statistics. Both the bias and the gain types of sensor fault were simulated to occur in the testing dataset. The comparison results using ROC curve showed that the new defined CCA-based statistics were the best and almost perfect fault detectors. Two special fault examples still showed that these two statistics could perfectly or successfully detect the corresponding sensor fault. In contrast, the PCA-based and the DPCA-based statistics did not perform on par. The fault isolation results also demonstrated that the faulty sensor was successfully identified through the new proposed fault isolation indices.

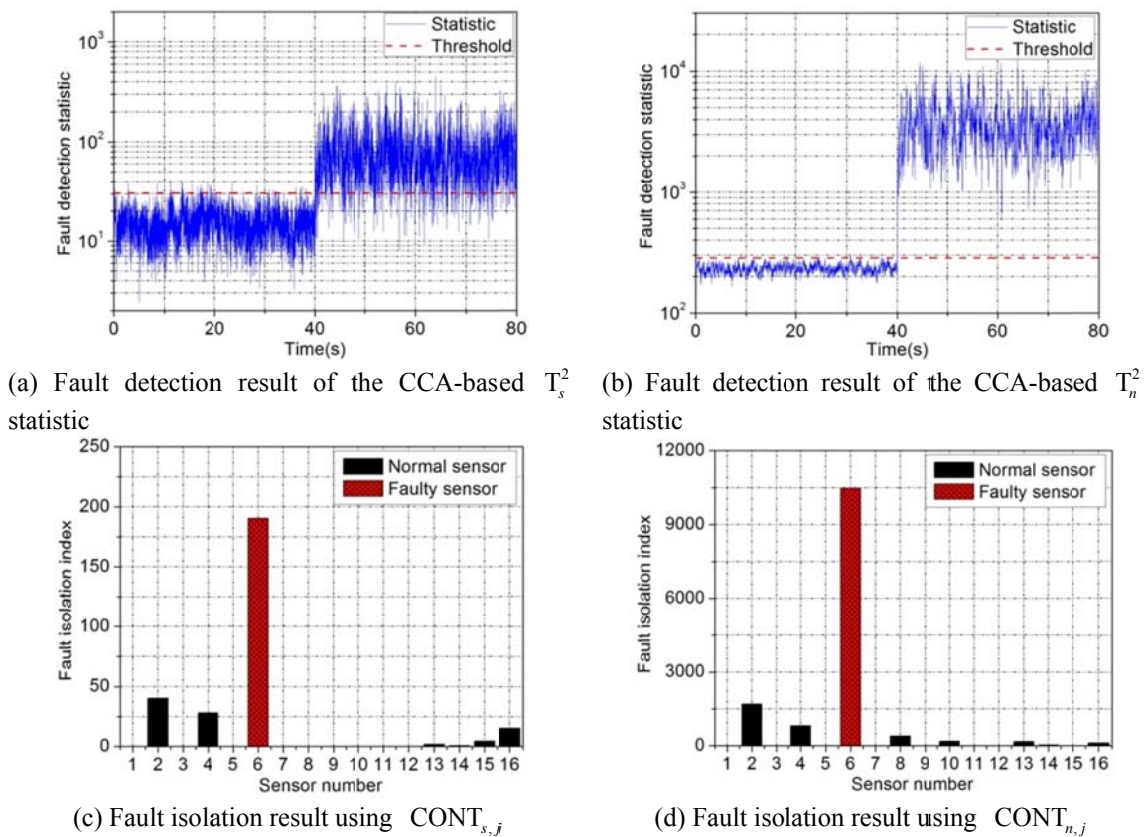


Fig. 10 Fault diagnosis results of the CCA-based method for the gain fault case

## Acknowledgments

This research work was jointly supported by the 973 Program (2015CB060000), the National Natural Science Foundation of China (51421064, 51478081), the Science Fund for Distinguished Young Scholars of Dalian (2015J12JH209), and the Fundamental Research Funds for Central Universities (DUT16LAB07).

## References

- Abdelghani, M. and Friswell, M.I. (2004), "Sensor validation for structural systems with additive sensor faults", *Struct. Health Monit.*, **3**(265), 265-275.
- Abdelghani, M. and Friswell, M.I. (2007), "Sensor validation for structural systems with multiplicative sensor faults", *Mech. Syst. Signal Pr.*, **21**(1), 270-279.
- Antoine, N. and Çınar, A. (1997), "Statistical monitoring of multivariable dynamic processes with state-space models", *Aiche J.*, **43**(8), 2002-2020.
- Catbas, F.N., Gul, M. and Burkett, J.L. (2008), "Damage assessment using flexibility and flexibility-based curvature for structural health monitoring", *Smart Mater. Struct.*, **17**(1), 015024.
- Chen, Q., Wynne, R.J., Goulding, P. and Sandoz, D. (2000), "The application of principal component analysis and kernel density estimation to enhance process monitoring", *Control Eng. Pract.*, **8**(5), 531-543.
- Chiang, L.H., Russell, E. and Braatz, R.D. (2001), *Fault detection and diagnosis in industrial systems*, Springer Verlag, London, UK.
- Correa, N.M., Adali, T., Li, Y.O. and Calhoun, V.D. (2010), "Canonical correlation analysis for data fusion and group inferences", *IEEE Signal Proc. Mag.*, **27**(4), 39-50.
- Dessi, D. and Camerlengo, G. (2015), "Damage identification techniques via modal curvature analysis: overview and comparison", *Mech. Syst. Signal Pr.*, **52-53**, 181-205.
- Erdogan, Y.S., Gul, M., Catbas, F.N. and Bakir, P.G. (2014), "Investigation of uncertainty changes in model outputs for finite-element model updating using structural health monitoring data", *J. Struct. Eng. - ASCE*, **140**(11), 04014078.
- Gul, M. and Catbas, F.N. (2011), "Damage assessment with ambient vibration data using a novel time series analysis methodology", *J. Struct. Eng. - ASCE*, **137**(12), 1518-1526.
- Hardoon, D.R., Szedmak, S. and Shawe-Taylor, J. (2003), "Canonical correlation analysis; an overview with application to learning methods", *Neural Computat.*, **16**(12), 2639-2664.
- Hernandez-Garcia, M.R. and Masri, S.F. (2014), "Application of statistical monitoring using latent-variable techniques for detection of faults in sensor networks", *J. Intell. Mat. Syst. Str.*, **25**(2), 121-136.
- Huang, H., He, H., Fan, X. and Zhang, J. (2010), "Super-resolution of human face image using canonical correlation analysis", *Pattern Recogn.*, **43**(7), 2532-2543.
- Huang, H.B., Yi, T.H. and Li, H.N. (2015), "Sensor fault diagnosis for structural health monitoring based on statistical hypothesis test and missing variable approach", *J. Aerospace Eng. - ASCE*, 10.1061/(ASCE)AS.1943-5525.0000572, B4015003.
- Huo, L., Song, G., Nagarajaiah, S. and Li, H. (2012), "Semi-active vibration suppression of a space truss structure using a fault tolerant controller", *J. Vib. Control*, **18**(10), 1436-1453.
- Karhunen, J., Hao, T. and Ylipaavalniemi, J. (2013), "Finding dependent and independent components from related data sets: a generalized canonical correlation analysis based method", *Neurocomputing*, **113**(7), 153-167.
- Kerschen, G., De Boe, P., Golinval, J.C. and Worden, K. (2005), "Sensor validation using principal component analysis", *Smart Mater. Struct.*, **14**(1), 36-42.
- Ku, W., Storer, R.H. and Georgakis, C. (1995), "Disturbance detection and isolation by dynamic principal

- component analysis”, *Chemometr. Intell. Lab.*, **30**(1), 179-196.
- Kullaa, J. (2010), “Sensor validation using minimum mean square error estimation”, *Mech. Syst. Signal Pr.*, **24**(5), 1444-1457.
- Lau, C., Ghosh, K., Hassain, M.A. and Hassan, C.R. (2013), “Fault diagnosis of Tennessee Eastman process with multi-scale PCA and ANFIS”, *Chemometr. Intell. Lab.*, **120**, 1-14.
- Li, H.N., Yi, T.H., Ren, L., Li, D.S. and Huo, L.S. (2014), “Reviews on innovations and applications in structural health monitoring for infrastructures”, *Struct. Monit. Maint.*, **1**(1), 1-45.
- Li, J. and Law, S.S. (2012), “Damage identification of a target substructure with moving load excitation”, *Mech. Syst. Signal Pr.*, **30**(7), 78-90.
- Li, J., Hao, H. and Lo, J.V. (2015), “Structural damage identification with power spectral density transmissibility: numerical and experimental studies”, *Smart. Struct. Syst.*, **15**(1), 15-40.
- Lu, Y. and Michaels, J.E. (2009), “Feature extraction and sensor fusion for ultrasonic structural health monitoring under changing environmental conditions”, *IEEE Sens. J.*, **9**(11), 1462 - 1471.
- Ni, Y.Q., Ye, X.W. and Ko, J.M. (2010), “Monitoring-based fatigue reliability assessment of steel bridges: analytical model and application”, *J. Struct. Eng.- ASCE*, **136**(12), 1563-1573.
- Ni, Y.Q., Ye, X.W. and Ko, J.M. (2012), “Modeling of stress spectrum using long-term monitoring data and finite mixture distributions”, *J. Eng. Mech.- ASCE*, **138**(2), 175-183.
- Pereira, D.A. and Serpa, A.L. (2015), “Bank of H-infinity filters for sensor fault isolation in active controlled flexible structures”, *Mech. Syst. Signal Pr.*, **60-61**, 678-694.
- Qin, S.J. (2003), “Statistical process monitoring: basics and beyond”, *J. Chemometr.*, **17**(8-9), 480-502.
- Rahbari, R., Niu, J., Brownjohn, J.M.W. and Koo, K.Y. (2015), “Structural identification of humber bridge for performance prognosis”, *Smart. Struct. Syst.*, **15**(3), 665-682.
- Roy, K., Bhattacharya, B. and Ray-Chaudhuri, S. (2015), “ARX model-based damage sensitive features for structural damage localization using output-only measurements”, *J. Sound Vib.*, **349**, 99-122.
- Sharifi, R., Kim, Y. and Langari, R. (2010), “Sensor fault isolation and detection of smart structures”, *Smart Mater. Struct.*, **19**(10), 105001.
- Smarsly, K. and Law, K.H. (2014), “Decentralized fault detection and isolation in wireless structural health monitoring systems using analytical redundancy”, *Adv. Eng. Softw.*, **73**, 1-10.
- Soman, R.N., Onoufrioua, T., Kyriakidesb, M.A., Votsisc, R.A. and Chrysostomou, C.Z. (2014), “Multi-type, multi-sensor placement optimization for structural health monitoring of long span bridges”, *Smart. Struct. Syst.*, **14**(1), 55-70.
- Sweeney, K.T., Mcloone, S.F. and Ward, T.E. (2013), “The use of ensemble empirical mode decomposition with canonical correlation analysis as a novel artifact removal technique”, *IEEE t. bio-med. Eng.*, **60**(1), 97-105.
- Thanagasundram, S., Spurgeon, S. and Schindwein, F.S. (2008), “A fault detection tool using analysis from an autoregressive model pole trajectory”, *J. Sound Vib.*, **317**(3), 975-993.
- The Mathworks (2014), MATLAB R2014a, Natick, Massachusetts, USA, <http://cn.mathworks.com>.
- Wang, H. and Song, G. (2011), “Fault detection and fault tolerant control of a smart base isolation system with magneto-rheological damper”, *Smart Mater. Struct.*, **20**(8), 298-300.
- Worden, K., Farrar, C.R., Haywood, J. and Todd, M. (2008), “A review of nonlinear dynamics applications to structural health monitoring”, *Struct. Control. Health.*, **15**(4), 540-567.
- Yamaguchi, H., Matsumoto, Y. and Yoshioka, T. (2015), “Effects of local structural damage in a steel truss bridge on internal dynamic coupling and modal damping”, *Smart. Struct. Syst.*, **15**(3), 523-541.
- Yi, T.H., Li, H.N. and Gu, M. (2011), “Optimal sensor placement for structural health monitoring based on multiple optimization strategies”, *Struct. Des. Tall Spec. Build.*, **20**(7), 881-900.
- Yi, T.H., Li, H.N. and Gu, M. (2013a), “Recent research and applications of GPS-based monitoring technology for high-rise structures”, *Struct. Control. Health.*, **20**(5), 649-670.
- Yi, T.H., Li, H.N. and Sun, H.M. (2013b), “Multi-stage structural damage diagnosis method based on ‘energy-damage’ theory”, *Smart. Struct. Syst.*, **12**(3-4), 345-361.
- Yi, T.H., Li, H.N. and Zhang, X.D. (2015a), “Sensor placement optimization in structural health monitoring using distributed monkey algorithm”, *Smart. Struct. Syst.*, **15**(1), 191-207.

Yin, S., Ding, S.X., Haghani, A., Hao, H. and Zhang, P. (2012), "A comparison study of basic data-driven fault diagnosis and process monitoring methods on the benchmark Tennessee Eastman process", *J. Process Contr.*, **22**(9), 1567-1581.